Computers in Biology and Medicine 113 (2019) 103393

Contents lists available at ScienceDirect

Computers in Biology and Medicine

journal homepage: www.elsevier.com/locate/compbiomed

Development of a personalized and realistic educational thyroid cancer phantom based on CT images: An evaluation of accuracy between three different 3D printers

Dayeong Hong[a], Sangwook Lee[a], Taehun Kim[a], Jung Hwan Baek[b], Yu-mi Lee[c], Ki-Wook Chung[c], Tae-Yon Sung[c,**,1], Namkug Kim[a,b,*,1]

[a] Department of Biomedical engineering, Asan Medical Institute of Convergence Science and Technology, Asan Medical Center, University of Ulsan College of Medicine, Seoul, 05505, Republic of Korea
[b] Department of Radiology, University of Ulsan College of Medicine, Asan Medical Center, Seoul, 05505, Republic of Korea
[c] Department of Surgery, University of Ulsan College of Medicine, Asan Medical Center, Seoul, 05505, Republic of Korea

ARTICLE INFO

Keywords:
3D printing
Thyroid cancer
Medical image
Phantom
Thyroidectomy

ABSTRACT

Background: Communication with patients on their thyroidectomy is complex and difficult, especially for inexperienced clinicians, because of the organ's anatomical complexity and proximity to arteries, veins, nerves and vital organs. The aim of this work was to develop a CT image-based 3D-printed model of thyroid cancer using various kinds of 3D printers and to compare their accuracies and other aspects regarding facilitating this patient-physician communication by improving both parties' understanding.

Methods: A 3D-printing model for thyroid surgery was designed based on head and neck CT data of a patient with thyroid cancer. Models reflecting the anatomical structure of the CT image were printed with three different types of 3D printers, namely, fused deposition modeling (FDM), color-jet printing (CJP), and Polyjet for comparison and evaluation. Appropriate printing materials and techniques were used to represent the texture and color of actual anatomical structures. Next, printing accuracies and various aspects of these phantoms were evaluated and compared to determine the advantages and disadvantages of the different printing types.

Results: Accuracies (mean difference ± 95% CI) of FDM, CJP, and Polyjet were 1.24 ± 0.77, 0.36 ± 0.34, and 0.58 ± 0.89 mm, respectively. Regarding accuracy and clinical demands, the Polyjet method was most suitable for fabricating an educational thyroid phantom; however, its cost was relatively high.

Conclusion: The phantoms produced could be used for various purposes, including teaching and training of less-experienced surgeons, for preoperative surgical planning and for patient education, and could provide more accurate and patient-specific anatomical information compared with commercially manufactured alternatives.

1. Introduction

In general, most thyroid cancers exhibit a favorable prognosis (> 90% 5-year disease-free survival) [1], and the frequency of tumor invasion to surrounding structures is low (< 15%) [2]. However, when the cancer invades, it can do so to important structures such as the trachea, esophagus, recurrent laryngeal nerve and major cervical arteries and veins [3,4]. In such highly advanced thyroid cancer cases, production of a thyroid phantom based on the CT images can help the patient and the surgeon understand the situation in many different ways [5,6].

Most industrial products are mass-produced and so have the same shape and size while, in contrast, medical patients have numerous differences in their anatomies. Therefore, 3D-printing technology could provide patient-specific products to meet medical needs [7–9]. The patient-specific phantom is one area of individualized medicine that has

* Corresponding author. Department of Radiology and Convergence Medicine , University of Ulsan College of Medicine, Asan Medical Center, 88 Olympic-ro 43 Gil, Songpa-gu, Seoul, 05505, South Korea.
** Corresponding author. Department of Surgery, University of Ulsan College of Medicine, Asan Medical Center, 88 Olympic-ro 43 Gil, Songpa-gu, Seoul, 05505, South Korea.
E-mail addresses: dyhong.89@gmail.com (D. Hong), Todltkddnr@gmail.com (S. Lee), taehun416@gmail.com (T. Kim), radbaek@naver.com (J.H. Baek), niphredil@amc.seoul.kr (Y.-m. Lee), surgeonckw@amc.seoul.kr (K.-W. Chung), tysung@amc.seoul.kr (T.-Y. Sung), namkugkim@gmail.com (N. Kim).
[1] These two authors contributed equally to this work.

https://doi.org/10.1016/j.compbiomed.2019.103393
Received 2 May 2019; Received in revised form 16 August 2019; Accepted 17 August 2019
Available online 18 August 2019
0010-4825/

Table 1
Descriptions of 3D-printing techniques.

Printing type	Additive manufacturing process
Fused deposition modeling (FDM)	FDM technology constructs objects layer-by-layer from the bottom up by heating and extruding thermoplastic filament. The process is somewhat similar to stereolithography, and specialized programs, or slicers, "cut" CAD models into layers and compute the manner in which the printer's extruder should assemble each layer.
Color-jet printing (CJP)	CJP uses a print head to selectively disperse a binder onto powder layers. The print head scans the powder tray and delivers a continuous jet of a solution that binds the powder particles together as it touches them.
Polyjet	Polyjet printing is performed by jetting a state-of-the-art photopolymer in ultra-thin layers of 16 μm onto a build tray layer-by-layer until the model is completed. Each photopolymer layer is cured by UV light immediately after it is jetted, producing fully cured models that can be handled and used immediately without any post-curing waiting period.

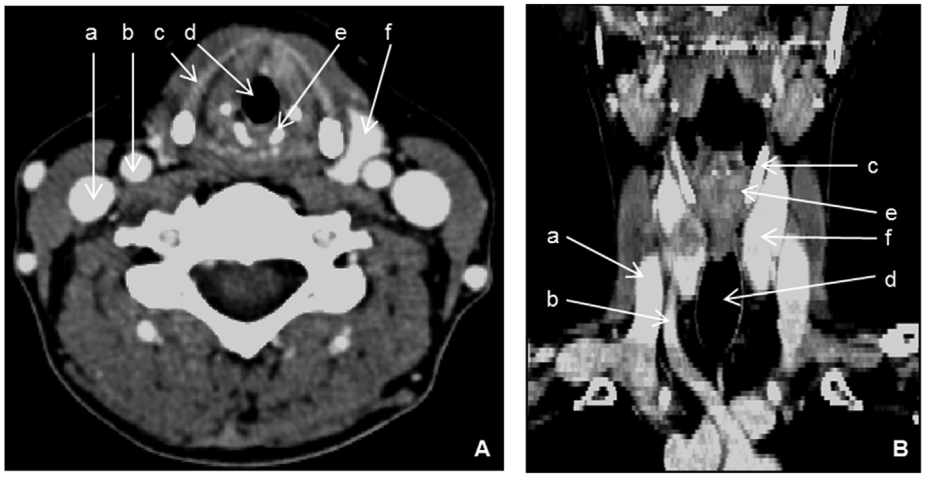

Fig. 1. Thyroid anatomy using head and neck CT. (a) Internal jugular vein, (b) common carotid artery, (c) thyroid cartilage, (d) trachea, (e) cricoid cartilage, and (f) thyroid.

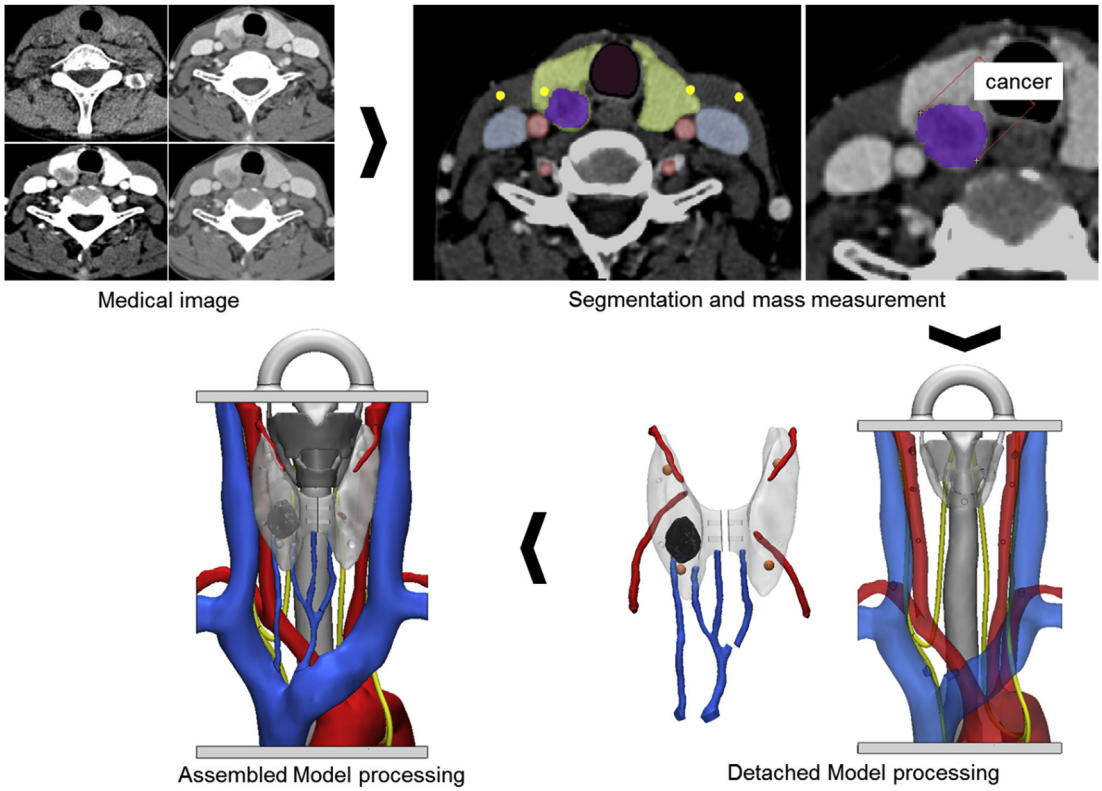

Fig. 2. Overall procedure for 3D modeling from medical images. The CT data from patient with thyroid cancer.

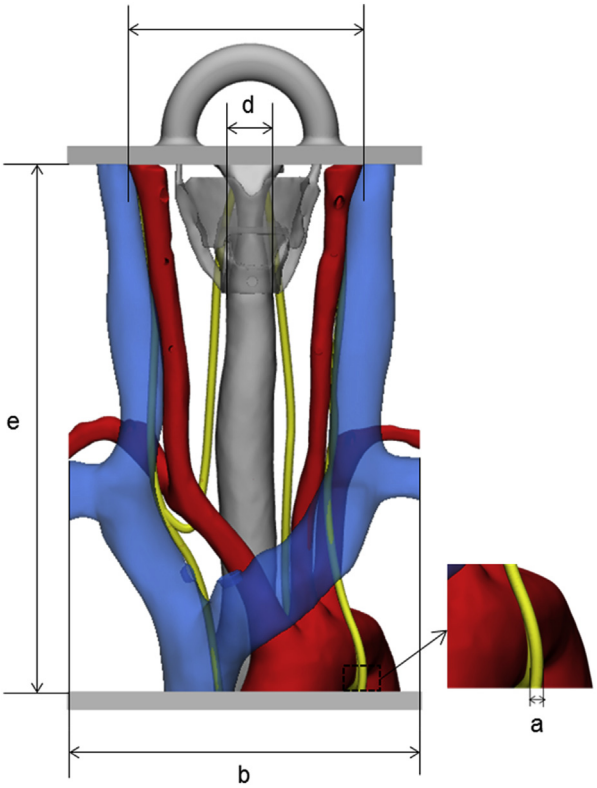

Fig. 3. The STL file with five landmarks specified for evaluating measurement error: (a) diameter of recurrent laryngeal nerve, (b) width of both veins, (c) width of both arteries, (d) diameter of the trachea, and (e) the distance between the upper and lower plates (arteries, red; veins, blue; nerve, yellow; trachea, gray).

been pioneered via the use of the 3D-printing concept and the procedure for phantom fabrication consists of multiple steps: (1) acquisition of high-quality CT data of the anatomical structure to be modeled, (2) image processing to extract the region of interest from the anatomic structure, (3) 3D modeling from medical doctor needs, (4) quality assurance of the model to ensure its accuracy, (5) Selection of printing method and materials, and (6) printing of the phantom [10].

Studies involving Patient-specific 3D-printed phantoms are remarkably few. Of these, Khalyfa et al. generated patient-specific bone implants and tissue engineering scaffolds [11], while Ryan et al. developed an aneurysm clipping simulacrum that supplements the training of neurosurgical residents who are learning to perform aneurysm surgery [12]. Furthermore, Bernhard et al. developed a kidney and tumor anatomy model for treatment planning, trainee teaching, and patient education [13].

Such studies have shown that patient CT data can be used to produce models suitable for 3D printing, and that such models can be used to predict pre-operative main vessel variation and to explain procedures to patients with a specific disease condition [14,15]. In this respect, a human CT-based thyroid cancer model would help in the education and understanding of individualized disease for both patients and their physicians. Therefore, we developed a 3D-printed model for thyroid cancer by using various kinds of 3D printer.

2. Methods

2.1. 3D-printing workflow

3D printing technology is particularly well suited to meet the increasing demand for cost-effective, high-quality patient-specific phantoms [16]. These can be used as visualization phantoms for either patient education or surgical simulation, and so it is important to consider the intended use when deciding which 3D-printing technology to use [17,18]. General consideration should be given to cost, quality, color, functional details, and printing time, which are dependent on the type and material of the printing technology. The most commonly used type are fused deposition modeling (FDM), color-jet printing (CJP), and Polyjet [19,20]. Table 1 shows a summary of the material and printing costs [21].

The development of various materials for 3D printing means that it can now be applied to various fields of medicine. However, it is important to consider the materials and technologies according in the light of medical needs [21]. In addition, researchers need to find ways to realize various materials by using the characteristics of materials [22].

2.1.1. CT scan protocols

The head and neck CT scan images of a patient with thyroid cancer who underwent MDCT (SOMATOM Definition Flash, Siemens Healthcare) based on the standard protocol of Asan Medical Center, Seoul, Korea, were retrospectively enrolled with the approval from the institutional review board (IRB). For 3D printing validation, each 3D printing phantom was scanned with the same CT protocol with 120 kVp and 1.0 mm slice thickness and reconstructed to 0.6 mm in the axial section by using a software (syngo CT 2012B). The final product was also scanned using the same CT and conditions.

2.1.2. Anatomical expertise

The important elements that need to be represented in a thyroid

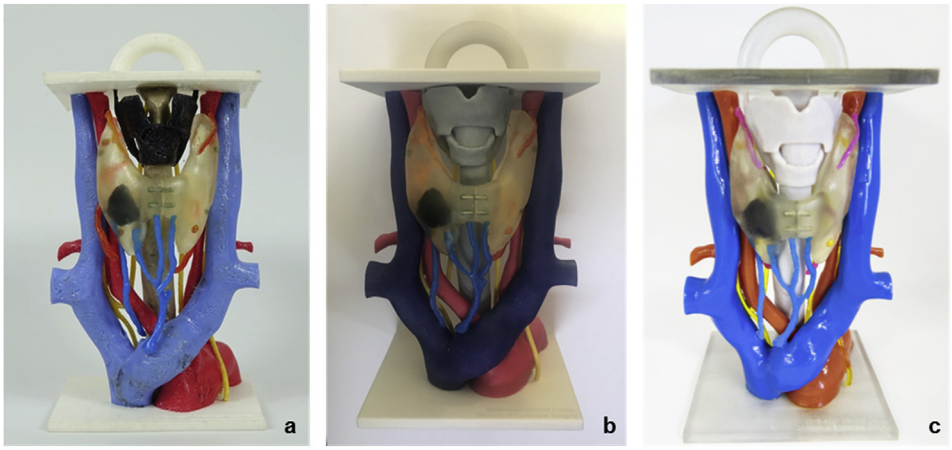

Fig. 4. Thyroid phantoms produced by three different 3D-printing techniques. (A) FDM, (B) CJP, and (C) Polyjet.

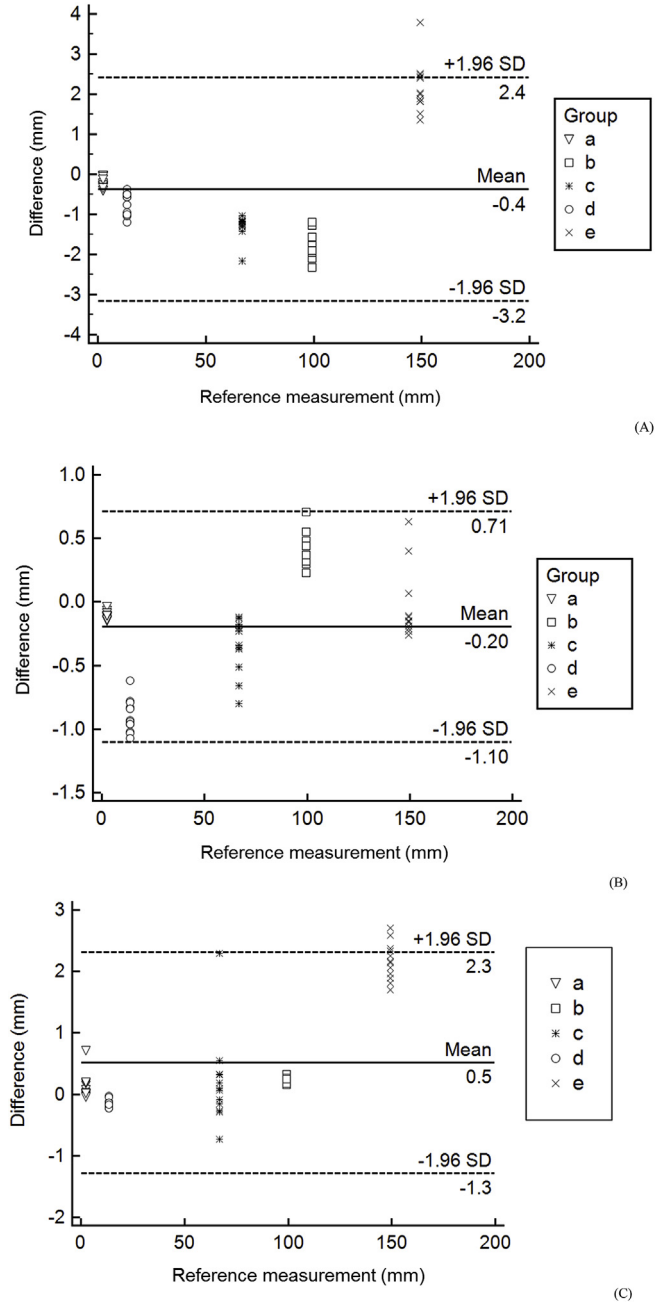

Fig. 5. The Bland-Altman analysis used to evaluate differences between the STL file (standard) and the three types of 3D-printed phantom. (A) STL vs FDM, (B) STL vs CJP, and (C) STL vs Polyjet. The chosen landmarks were (a) the diameter of recurrent laryngeal nerve, (b) width of both veins, (c) width of both arteries, (d) diameter of the trachea, and (e) the distance between the upper and lower plates.

Table 2
Comparison of the reference measurements between the three types of 3D-printed thyroid phantoms.

Reference measurement – Thyroid phantom	3D-printing method		
	FDM	CJP	Polyjet
mean absolute difference (mm)	1.24 ± 0.77	0.36 ± 0.34	0.58 ± 0.89
mean relative difference (%)	4.00 ± 3.41	2.36 ± 2.92	1.51 ± 1.72

FDM = fused deposition modeling, CJP = color-jet printing.

gland model are the jugular veins, common carotid artery, thyroid cartilage, cricoid cartilage, trachea, parathyroid gland, thyroid gland, tumor, and recurrent laryngeal nerves (Fig. 1) [23,24].

Certain structures surrounding the thyroid gland are very important regarding their functional roles. When to thyroid cancer invades the jugular vein or carotid artery, the vessels need to be ligated to perform a curative surgical resection, which could result in restricted blood flow to and from the brain, while tracheal invasion might require tracheal resection to prevent airway obstruction. Recurrent laryngeal nerve invasion may result in changes to the voice and, in addition, render the nerve nonfunctional; these situations may result in permanent voice impairment after surgery. In this study, recurrent laryngeal nerve and parathyroid were created with reference to the existing anatomical structure. However, more detailed anatomic structures are needed to be designed with the aid of additional images from MRI and ultrasound to recognize subtle structures in the CT image. Therefore, awareness of such structural variations from using 3D thyroid modeling of the deformity before surgery will help to minimize unexpected post-operative complications by more educated pre-operative planning.

2.1.3. Procedure for 3D printing

Fig. 2 shows the procedure implemented for printing of the thyroid phantoms.

Head and neck CT images were segmented and modeled using the medical image processing software Mimics and 3-matics (Materialise, Leuven, Belgium). The segmentation took within 3 h by an operator (DYHong), excluding the time on updating the segmentation as requested by a surgeon.

Major anatomical structures related to thyroid cancer were segmented and modeled for phantom production. Each structure was segmented directly from human CT data. The common carotid artery, which has relatively clear pathways and CT values, was easily segmented using the region growing function. In contrast, nerves and the parathyroid, which do not exhibit clear shapes on the CT, were modeled by referring to the anatomical structure [25]. The patient's CT data were segmented and modeled by an expert, and the results were confirmed by a radiologist and a surgeon with more than 15 years of experience.

The completed modeling file was converted into an STL format file that can be 3D printed (Fig. 2).

Printing utilized three 3D-printing methods and materials, namely the FDM, CJP and Polyjet methods. The texture and esthetics of the final printed models were discussed with a clinician.

2.1.4. Comparison of accuracy between the STL file and the three types of 3D-printed phantoms

The phantom was output to three types of printers from the same STL file. To compare the accuracy of each 3D-printed phantom with that of the original file, we assigned the same landmarks to five locations, and two researchers measured them 5 times each, for a total of 10 times (Fig. 3), using Vernier calipers. A Bland–Altman analysis was used to evaluate the STL file and printed phantom using MedCalc software (trial version 18.2.1). Paired *t*-test was used to compare the differences between STL file and the three types of phantom using the SPSS software (trial version 25.00; IBM) was collected and important structures were segmented. The segmented data was modeled in an assembled form so that either a total or partial thyroidectomy could be implemented. Each structure was rendered in a different color.

3. Results

The main components that must be represented in a thyroid phantom are the internal jugular veins, trachea, common carotid arteries, major cartilage, thyroid gland, tumor, parathyroid, and recurrent laryngeal nerves. All these components were 3D-printed to produce a single model, while the thyroid gland structures were produced as a

Table 3
A comparison of 3D-printing technologies.

Type	Materials	Multi-color	Multi-Materials	Transparency	hardness (HA)	Cost
FDM	TPE	No limit	Impossible	Impossible	56.5	Low
CJP	Plasters	RGB	Impossible	Impossible	94.0	Middle
Polyjet	Photopolymers	No limit	Possible	Relies on materials (agilus, tango)	79.6	High

FDM = fused deposition modeling, CJP = color-jet printing.

Table 4
A comparison of thyroid phantoms produced by various 3D-printing methods.

Type	Cost (USD)	Printer (company)	Printing time (hours)	Materials
FDM	35.40	Good boT 1236 M, 3D KOREA, Inc.	65	TPE
CJP	225.67	ProJet CJP 660Pro, 3DSystmes, Inc.	7	Visijet PXL
Polyjet	474.01	Objet J750, Stratasys, Inc.	18.5	Vero series

FDM = fused deposition modeling, CJP = color-jet printing, 3D = three-dimensional.

Table 5
Evaluation by a surgeon; pros and cons of 3 phantom types.

	FDM	CJP	Polyjet
Advantage	Not fragile	Multi-colored	Multi-colored Smooth surface Detachable anatomy
Disadvantage	Unclear surface	Fragile Rough surface	–

FDM = fused deposition modeling, CJP = color-jet printing.

separate, detachable model.

TangoPlus (Stratasys Ltd.) is more transparent than the other materials; therefore, it was used for the fabrication of a thyroid gland. In addition, small vessels connected to the thyroid gland required the fabrication of thin, narrow structures, and TangoPlus was mixed for their fabrication [26].

Three phantom models were produced using three types of 3D-printing techniques (Fig. 4), and to evaluate their representational accuracy, two researchers measured five individual metrics for five times each to produce 10 measurements per metric in total.

The corresponding metrics in the original STL file were compared to the physical measurements and evaluated using a Bland–Altman plot (Fig. 5 and Table 2). In the 3D printing with FDM, the mean ± standard deviation (SD) of the differences was 1.24 ± 0.77 mm (limits of agreement from −3.2 to 2.4 mm) (Fig. 5A), whereas in the 3D printing with CJP, 0.36 ± 0.34 mm (limits of agreement from −1.10 to 0.71 mm) was obtained (Fig. 5B). Additionally, the mean ± SD of the differences of the Polyjet printed parts was 0.58 ± 0.89 mm (limits of agreement from −1.3 to 2.3 mm) (Fig. 5C). All the measurements, except for the distance between the upper and lower plates (Fig. 3e), were within the 95% confidence interval. Furthermore, the order of accuracy of the three types was as follows: CJP > Polyjet > FDM. In the case of CJP, the mean difference of the distance between the upper and lower plates was −0.04 mm; meanwhile, the mean difference of the FDM-type phantom was smaller than that in the STL file. The Polyjet model had a delicate error in two measurement values, but the value was reliable.

In addition, advantages and disadvantages of the three printing methods were clearly revealed (Table 3). FDM printing was more economical than others but had disadvantages regarding processing and hardness. Additionally, CJP printing was the fastest of the three printer types tested (Table 4); however, the resulting model was unsuitable for use as an education phantom because the thin anatomic structures were easily broken. Polyjet printing was the costliest but met the quality needs required for medical use.

We analyzed the strengths and weaknesses of the three type of printed model and evaluated their value as educational phantoms from the perspective of surgeon (Table 5).

4. Discussion

CJP, FDM, and Polyjet are typical 3D printing techniques used to print multicolored models, which could be essential for educational phantoms. For the educational purpose, the mean absolute difference (about 1.2 mm) of FDM could be used for explaining the size, shape and

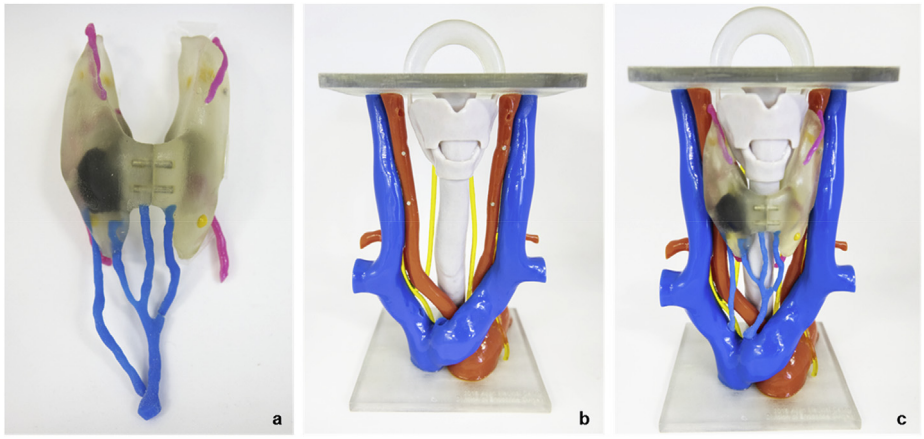

Fig. 6. Final thyroid phantom model. (A) Thyroid region with small vessels and parathyroid. (B) Other regions with main vessels, nerves, trachea, and cartilage. (C) Final modeling of the two-part phantom.

location of the lesions and their relationship with the surrounding structures. More important factors for education are material properties of 3D printing including colors, transparency, softness, and surface finishing. Considering the Bland–Altman plot, CJP and Polyjet are the most useful. However, the thin parts printed by CJP were easily broken and difficult to post-process. Polyjet is more suitable for educational phantoms than CJP due to its favorable physical properties and robustness. Especially, the error of the distance between the upper and lower plates was estimated as the printing error of the equipment and can be overcome through the printing direction and the temperature.

As a result of the above findings, we recommend Polyjet printing (Polyjet J750; Stratasys, Eden Prairie, MN) using photopolymers for the production of thyroid medical phantoms (Fig. 6). This printing technique can produce the colors desired by the clinician and can also be printed with transparent materials so that the interior of the thyroid, where the lesion is located, can be seen. The hardness of each part can also be adjusted by mixing the materials. The upper and lower plates can also be printed out transparently, helping the patient to understand their pathology while and heightening the aesthetics of the structure. This study aimed at producing an educational phantom in which patient-specific manufacturing is unnecessary; thus, the cost and printing time of this model are not influenced considerably, contrary to a surgical guide and a simulator that need to be manufactured individually for each patient.

Fig. 6 shows the assembled and Polyjet printed thyroid phantom implemented in this study. Its configuration was similar to that of the model reconstructed from human CT data. Both lobes of the thyroid are designed to be detached and, for the protection of the phantom, the attachment mechanism was designed to be magnetic.

The phantom will be used for pre-operative and post-operative training of patients, and its clinical value will be assessed by conducting questionnaires on its educational usefulness from the viewpoint of patients and physicians.

In this study has several limitations. It is the first study to make a personalized and realistic thyroid cancer phantom for patient education by using medical image and various kinds of 3D printers in actual clinical environment between clinician and patients. Therefore, we compared their accuracies and other aspects regarding facilitating this patient-physician communication by improving both parties' understanding. In addition, the phantom in the study may have an anatomic limitation because it was obtained from a single patient with thyroid cancer [19]. Therefore, a future study will produce patient-specific phantoms from a number of patients and from those with other diseases and obtain more realistic representation and verification of the anatomical structure, possibly by adding cadaver or animal studies. Even though we were able to a patient-specific phantom based on CT images of a patient, it was difficult to reproduce structures such as nerves, which are rarely observed in medical imaging, including CT, and these needed to be reproduced with limited knowledge. Because the main aim of this study is to fabricate an adequate educational thyroid phantom in actual clinical environment, the use of the phantom may not affect the selection of patient treatment options. In the long run, this phantom could be used for a rehearsal simulation or a surgical guide of more accurate partial thyroidectomy. In addition, multiple landmarks of the three different types of thyroid phantoms measured by Vernier calipers were compared with their corresponding points in the original STL modeling file. Hence, we used the Bland–Altman method, but the distance error map on each point insufficiently evaluated the accuracies of our phantoms. For further study, CT or laser surface scans will be needed to evaluate the distance error map. Polyjet printing technology is useful for fabricating an educational phantom because it can control hardness by mixing certain amounts of the printing materials. However, this technology has limitations in recognizing realistic human physical properties. Hence, further research is needed to develop materials that can reflect human physical properties more accurately. Furthermore, the physical properties need to be implemented by properly controlling the silicone and the newly developed 3D printing materials [27].

5. Conclusion

In conclusion, the phantom produced in this study can be used in educating patients with common thyroid diseases, allowing them to understand their illness better, and by surgeons to allow them to plan a complex surgery in advance. Especially, having a 3D phantom of advanced thyroid cancer prior to surgery could be useful in minimizing unsuspected injury to the organs that should be kept intact throughout the operation and decreasing the chance of postoperative complications. It could also allow the surgeons to thoroughly plan the procedure preoperatively if the invaded surrounding structures require a complex reconstruction. Furthermore, constructs such as vessels, tissues, and cervical spines could be implemented using agar and silicone. Such improvements could be applied for use in a basic airway intubation simulator but also to phantoms that could be used for surgical practice for rare and difficult cases, such as cricothyroidotomy [28,29].Three-dimensional printing technology provides more anatomic information that differs from currently available thyroid models, enabling more effective patient consultations, improved diagnostic quality, and improved surgical planning. In addition, as 3D-printing technology evolves further, tissues or organs might one day even be produced using 3D-printing methods. Thus, 3D-printing technology has the potential to be of great benefit to medicine in terms of patient-specific individualization. In the future, aside from 3D printing technology, virtual reality and augmented reality technologies could be applied for clinical education, given its economic costs, as well as patient-specific thyroidectomy education.

Funding

This research did not receive any specific grant from funding agencies in the public, commercial, or not-for-profit sectors.

Conflicts of interest

We conducted our own research without any financial support. If there is a problem with this part, we will be entirely responsible.

Acknowledgements

we would like to thank Minkyoung Kim for her excellent technical assistance and graphical abstracts making.

References

[1] Mingzhao Xing, et al., BRAF mutation predicts a poorer clinical prognosis for papillary thyroid cancer, J. Clin. Endocrinol. Metab. 90 (12) (2005) 6373–6379.
[2] Donald SA. McLeod, et al., Prognosis of differentiated thyroid cancer in relation to serum thyrotropin and thyroglobulin antibody status at time of diagnosis, Thyroid 24 (1) (2014) 35–42.
[3] Ernest L. Mazzaferri, Sissy M. Jhiang, Long-term impact of initial surgical and medical therapy on papillary and follicular thyroid cancer, Am. J. Med. 97 (5) (1994) 418–428.
[4] Masahiro Ohgami, et al., Scarless endoscopic thyroidectomy: breast approach for better cosmesis, Surg. Laparosc. Endosc. Percutaneous Tech. 10 (1) (2000) 1–4.
[5] Fabian Rengier, et al., 3D printing based on imaging data: review of medical applications, Int. J. Computer. Assist. Radiol. Surgery. 5 (4) (2010) 335–341.
[6] C. Lee Ventola, Medical applications for 3D printing: current and projected uses, Pharm. Therapeut. 39 (10) (2014) 704.
[7] Alaadien Khalyfa, et al., Development of a new calcium phosphate powder-binder system for the 3D printing of patient specific implants, J. Mater. Sci. Mater. Med. 18 (5) (2007) 909–916.
[8] Justin R. Ryan, et al., Cerebral aneurysm clipping surgery simulation using patient-specific 3D printing and silicone casting, World neurosurgery 88 (2016) 175–181.
[9] Mazher Mohammed, et al., Customised design and development of patient specific 3D printed whole mandible implant, Proceedings of the 27th Annual International Solid Freeform Fabrication Symposium, 2016.
[10] Dimitris Mitsouras, et al., Medical 3D printing for the radiologist, RadioGraphics 35 (7) (2015) 1965–1988.

[11] Alaadien Khalyfa, et al., Development of a new calcium phosphate powder-binder system for the 3D printing of patient specific implants, J. Mater. Sci. Mater. Med. 18 (5) (2007) 909–916.
[12] Justin R. Ryan, et al., Cerebral aneurysm clipping surgery simulation using patient-specific 3D printing and silicone casting, World neurosurgery 88 (2016) 175–181.
[13] Jean-Christophe Bernhard, et al., Personalized 3D printed model of kidney and tumor anatomy: a useful tool for patient education, World J. Urol. 34 (3) (2016) 337–345.
[14] Jiang Hsieh, Computed Tomography: Principles, Design, Artifacts, and Recent Advances, SPIE, Bellingham, WA, 2009.
[15] Daniela Nascimento Silva, et al., Dimensional error in selective laser sintering and 3D-printing of models for craniomaxillary anatomy reconstruction, J. Cranio-maxillofacial. Surgery. 36 (8) (2008) 443–449.
[16] Di Prima, Matthew, et al., Additively manufactured medical products–the FDA perspective, 3D printing in medicine 2 (1) (2015) 1.
[17] Yousef AbouHashem, et al., The application of 3D printing in anatomy education, Med. Educ. Online 20 (1) (2015) 29847.
[18] Theodore L. Gerstle, et al., A plastic surgery application in evolution: three-dimensional printing, Plast. Reconstr. Surg. 133 (2) (2014) 446–451.
[19] P.F.D.M. Dudek, FDM 3D printing technology in manufacturing composite elements, Arch. Metall. Mater. 58 (4) (2013) 1415–1418.
[20] Michael W. Barclift, Christopher B. Williams, Examining variability in the mechanical properties of parts manufactured via Polyjet direct 3D printing, International Solid Freeform Fabrication Symposium, University of Texas at Austin, Austin, Texas, 2012.
[21] Guk Bae Kim, et al., Three-dimensional printing: basic principles and applications in medicine and radiology, Korean J. Radiol. 17 (2) (2016) 182–197.
[22] Sung Yong Hong, et al., Experimental investigation of mechanical properties of UV-Curable 3D printing materials, Polymer 145 (2018) 88–94.
[23] Claudio R. Cernea, et al., Surgical anatomy of the external branch of the superior laryngeal nerve, Head Neck 14 (5) (1992) 380–383.
[24] Sara L. Richer, Barry L. Wenig, Changes in surgical anatomy following thyroidectomy, Otolaryngol. Clin. N. Am. 41 (6) (2008) 1069–1078.
[25] Richard D. Bliss, Paul G. Gauger, Leigh W. Delbridge, Surgeon's approach to the thyroid gland: surgical anatomy and the importance of technique, World J. Surg. 24 (8) (2000) 891–897.
[26] Mazher Iqbal Mohammed, et al., Advanced auricular prosthesis development by 3D modelling and multi-material printing, KnE Engineering 2 (2) (2017) 37–43.
[27] Justin R. Ryan, et al., Cerebral aneurysm clipping surgery simulation using patient-specific 3D printing and silicone casting, World neurosurgery 88 (2016) 175–181.
[28] Christopher K. Salvino, et al., Emergency cricothyroidotomy in trauma victims, J. Trauma 34 (4) (1993) 503–505.
[29] Jacob Melchiors, et al., Preparing for emergency: a valid, reliable assessment tool for emergency cricothyroidotomy skills, Otolaryngology-Head Neck Surg. (Tokyo) 152 (2) (2015) 260–265.